33p

N63-15323

code-1

NASA

TECHNICAL NOTE

D-1894

ON THE FLOW STRUCTURE WITHIN A CONSTANT PRESSURE

COMPRESSIBLE TURBULENT JET MIXING REGION

By W. L. Chow and H. H. Korst

NATIONAL AERONAUTICS AND SPACE ADMINISTRATION

WASHINGTON   April 1963

Code-1

NATIONAL AERONAUTICS AND SPACE ADMINISTRATION

TECHNICAL NOTE D-1894

ON THE FLOW STRUCTURE WITHIN A CONSTANT

PRESSURE COMPRESSIBLE TURBULENT

JET MIXING REGION

By W. L. Chow and H. H. Korst

SUMMARY

/ 5-3-23

Results are presented from the numerical calculations carried out to produce detailed information on the kinematic, dynamic, dissipative, and thermodynamic characteristics of a uniform half infinite stream, mixing with a quiescent fluid of the same composition.

An effective Prandtl number of $Pr_t = 1$ is assumed for the constant pressure, non-isoenergetic turbulent mixing process.

The ratio of specific heat becomes absorbed by selecting Crocco number instead of Mach number as measure for the compressibility, thus allowing generalization of the results to any perfect non-reacting gas having constant specific heat.

After identifying a functional form for the streamwise component of the velocity profile, a single empirical mixing parameter becomes well defined and can be absorbed in a rational presentation of structural details of jet mixing regions, such as the vertical velocity component, temperature and density distribution, integrals describing flow of mass, momentum, mechanical energy, the transfer of shear work and heat across individual streamlines, as well as local and integrated dissipation rates for mechanical energy.

Information on the empirical parameter σ remains generally incomplete. Although values for low-speed isoenergetic mixing are well established and effects of Mach number have been tentatively reported, no such information is presently available for temperature level and temperature differential influence.

SYMBOLS

C_f	friction coefficient
C_p	specific heat at constant pressure
C	$C = \dfrac{u}{\sqrt{2C_p T_o}}$ Crocco number
M	Mach number
Pr_t	turbulent Prandtl number
St	Stanton number
T	absolute temperature
u	velocity component in x – direction
v	velocity component in y – direction
x,y	coordinates in the intrinsic coordinate system
X,Y	coordinates in the reference coordinate system
ϵ	eddy diffusivity
η_p	position parameter
η_m	dimensionless shift of the intrinsic system of coordinates with respect to reference coordinate system
η	$\eta = \sigma \dfrac{Y}{x}$
Λ	$\Lambda = \dfrac{T_o}{T_{oa}}$ the stagnation temperature ratio
ρ	mass density
σ	similarity parameter for the homogeneous coordinate system
τ_t	turbulent shear stress
φ	$\varphi = \dfrac{u}{u_a}$ dimensionless velocity
φ'	$\varphi' = \dfrac{v}{u_a}$

2

Ω Energy transport rate per unit width and per unit length along the jet mixing region.

Subscripts

a   refers to conditions in the free stream adjacent to dissipation regions

b   refers to wake conditions (near base)

j   refers to jet boundary streamline

l   refers to local position

o   refers to stagnation value

Auxiliary integrals and functions

$$I_1 \left[C_a{}^2, \frac{T_b}{T_{oa}}, \eta \right] \equiv \int_{-\infty}^{\eta} \frac{\varphi}{\Lambda - C_a{}^2 \varphi^2} \, d\eta$$

$$I_2 \left[C_a{}^2, \frac{T_b}{T_{oa}}, \eta \right] \equiv \int_{-\infty}^{\eta} \frac{\varphi}{\Lambda - C_a{}^2 \varphi^2} \, d\eta$$

$$I_3 \left[C_a{}^2, \frac{T_b}{T_{oa}}, \eta \right] \equiv \int_{-\infty}^{\eta} \frac{\Lambda \varphi}{\Lambda - C_a{}^2 \varphi^2} \, d\eta$$

$$I_4 \left[C_a{}^2, \frac{T_b}{T_{oa}}, \eta \right] \equiv \int_{-\infty}^{\eta} \frac{\varphi^3}{\Lambda - C_a{}^2 \varphi^2} \, d\eta$$

E   auxiliary dimensionless energy transfer function

$$E \equiv [I_1(\eta_R) - I_1(\eta_j)] - [I_3(\eta_R) - I_3(\eta_j)]$$

W_s local shear work

$$W_s \equiv \frac{\tau_t \, u \, \sigma}{\rho_a u_a{}^3}$$

θ_D local dissipation function

$$\theta_D \equiv \frac{\tau_t \frac{\partial u}{\partial y} \, x}{\rho_a u_a{}^3} \equiv \frac{\theta_d \, x}{\rho_a u_a{}^3}$$

τ shear stress function

$$\tau = \frac{\tau_t \, \sigma}{\rho_a u_a{}^2}$$

ϕ total rate of dissipation of mechanical energy per unit length

$$\phi = \frac{\sigma \int_{-\infty}^{\infty} \tau_t \frac{\partial u}{\partial y} \, dy}{\rho_a u_a^{\ 3}} = \frac{x \int_{-\infty}^{\infty} \theta_d \, d\eta}{\rho_a u_a^{\ 3}}$$

ε eddy diffusivity function

$$\varepsilon = \frac{c \, \sigma^2}{x \, u_a}$$

4

Introduction

The interest in flow problems involving separation from solid boundaries leads to studies of the flow mechanism in the wake, and its component flow regions.

Significant wake flow components may be identified as:

i) the flow field near the separation point,
ii) the jet mixing component between the wake and the adjacent free stream,
iii) the region of reattachment (often recompression) at the end of the wake,
iv) the flow field within the wake,
v) the redevelopment of the flow field downstream of the end of the wake.

Understanding of wake dynamics has benefited greatly from the analysis of such wake flow components, as evidenced by the treatment of the classical base pressure problem and its ramifications (ref. 1). The jet mixing component is of special importance in its contribution to wake flow mechanisms, and has, therefore, received wide attention in the literature.

Mixing between a uniform stream and a quiescent fluid, as well as mixing involving two streams have been studied extensively both analytically and experimentally.* Yet, even, the most fundamental and simplest information, e.g. concerning the influence of compressibility and temperature level on the effective turbulent eddy viscosity in turbulent jet mixing regions is still subject to searching speculations (ref. 4). While it appears logical to draw such information from an analysis of experimental data on mixing profiles, in concentrating on the vicinity of the inflection point tangent, and to observe the close relationships between the functional presentation of a mixing profile and the resulting definition of an empirical mixing parameter, such an approach has, so far, not been uniformly accepted. After identifying a functional form for the velocity profile, such a single empirical parameter becomes well defined and can be utilized in a rational presentation even of detailed information on jet mixing regions. Final identification by numerical values may still have to depend on further empirical information on this mixing parameter. The present communication is concerned with the turbulent, compressible constant pressure mixing problem,

---

*The rapid rate at which contributions are being made to these fields forces one to look beyond the treatments and references included in such standard works as by Schlichting (ref. 2) and Pai (ref. 3) and to survey the current literature.

resulting from interaction between a uniform stream and a quiescent wake, both having the same composition, but, in general, different stagnation temperature and an effective turbulent Prandtl Number of unity. Detailed information is given on the kinematic, dynamic, dissipative and thermodynamic structure of such jet mixing regions. The use of Crocco Number as parameter for compressibility effects eliminates the influence of the specific heat ratio, and thus, permits a wider utilization of the results (ref. 5). It shall be noted that jet mixing between a uniform stream and a quiescent fluid serves satisfactorily as a flow component in many problems concerned with wake dynamics. Thermodynamic analysis of separated flow regions and a study of the mechanism of energy transfer to and across wakes requires however the consideration of finite entrainment velocities in the jet mixing component (ref. 6). A subsequent report similar in scope to the present one, will present information on the two-stream jet mixing problem.*

In the study of the flow mechanism and heat transfer in separated flow problems, it is necessary to study the detailed local properties within such turbulent jet mixing regions which would be helpful to understand the basic flow mechanisms and identify the controlling components within such separated flow regions.

The present work is essentially a logic extension of previous investigations conducted at the University of Illinois, which utilized an integral momentum approach to obtain theoretical solutions for the isoenergetic (ref. 5, 7) and non-isoenergetic (ref. 8, 9) compressible turbulent jet mixing problem. In order to have consistent presentation, the previous work on which the present analysis is based will be first summarized and reviewed.

---

*A comprehensive computation program has been carried out at the University of Illinois under the NASA Grant NsG-13-59 and samples have been presented in ref.6.

6

Theoretical Analysis

The differential equation of motion for a constant pressure turbulent jet mixing region was highly simplified and solved through an integral transformation by extending Prandtl's exchange coefficient concept. The solution was written as functions of the initial disturbed profile as well as the "position parameter η_p". (Ref. 5). It was shown that in the case of small initial disturbance or at a location far downstream, the velocity profile would asymptotically reach one termed as "fully developed", ($\eta_p = 0$) which is no longer dependent upon the initial disturbed profile.

For a turbulent Prandtl Number of one ($Pr_t = 1$), the Crocco integral energy relationship will relate the stagnation temperature profile throughout such a mixing region uniquely to the velocity profile. (Ref. 9).

The solution for the flow field in the mixing region thus obtained was interpreted to hold in an intrinsic coordinates system (x,y) which was subsequently localized with respect to the reference coordinate system (X, Y) by a momentum integral relationship. In the following, all equations are written for the "fully developed" profiles within such a constant pressure compressible non-isoenergetic turbulent jet mixing region.

Jet Mixing Profile

The dimensionless velocity profile is given by

$$\varphi = \tfrac{1}{2} (1 + erf\ \eta) \tag{1}$$

where

$$\varphi = \frac{u}{u_a}$$

$$erf\ \eta = \frac{2}{\sqrt{\pi}} \int_0^{\eta} e^{-\beta^2} d\beta$$

$$\eta = \sigma \frac{y}{x}$$

and σ is the similarity parameter for the homogeneous coordinate system. A discussion of the parameter σ as identified for the error function velocity distribution is given in Appendix A.

The stagnation temperature profile is given by

$$\Lambda = \frac{T_o}{T_{oa}} = \frac{T_b}{T_{oa}} + (1 - \frac{T_b}{T_{oa}}) \; \varphi \qquad (2)$$

The dimensionless shift η_m of the "intrinsic system of coordinates" with respect to the reference coordinate system is given by

$$\eta_m = \eta_R - (1 - c_a^2) \int_{-\infty}^{\eta_R} \frac{\varphi^2}{\Lambda - c_a^2 \varphi^2} \; d\eta \qquad (3)$$

where η_R is a large value of η such that

$$1 - \varphi \; (\eta_R) < t$$

$$\text{and} \quad \left| \; 1 - \Lambda \; (\eta_R) \; \right| < t'$$

t and t' being small quantities.

Auxiliary Integrals

The integrals related to this analysis are defined and listed as follows:

$$I_1 \; (c_a^2, \frac{T_b}{T_{oa}}, \eta) \equiv \int_{-\infty}^{\eta} \frac{\varphi}{\Lambda - c_a^2 \varphi^2} \; d\eta$$

$$I_2 \; (c_a^2, \frac{T_b}{T_{oa}}, \eta) \equiv \int_{-\infty}^{\eta} \frac{\varphi^2}{\Lambda - c_a^2 \varphi^2} \; d\eta$$

$$I_3 \; (c_a^2, \frac{T_b}{T_{oa}}, \eta) \equiv \int_{-\infty}^{\eta} \frac{\Lambda \; \varphi}{\Lambda - c_a^2 \varphi^2} \; d\eta*$$

---

*Note that this integral I_3 has been defined as I_2 in Refs. 1 and 9.

8

$$I_4 \left(C_a^2, \frac{T_b}{T_{oa}}, \eta \right) \equiv \int_{-\infty}^{\eta} \frac{\varphi^3}{\Lambda - C_a^2 \varphi^2} \, d\eta$$

For fixed values of C_a^2 and $\frac{T_b}{T_{oa}}$, these integrals may be represented in short by $I_1(\eta)$, $I_2(\eta)$, $I_3(\eta)$ and $I_4(\eta)$ respectively.

Jet Boundary Streamline

The "jet boundary streamline" which separates the fluid of the external stream from the fluid entrained within the wake is identified by η_j which satisfies:

$$I_1(\eta_R) - I_1(\eta_j) = I_2(\eta_R) \tag{4}$$

Energy Transfer

The energy transferred across the "jet boundary streamline" is given by $\mathcal{Q}$ which satisfies

$$\frac{\mathcal{Q} \, \sigma}{c_p \rho_a u_a (T_{oa} - T_b)} = St \times \sigma = (1 - C_a^2) \, E/1 - \frac{T_b}{T_{oa}} \tag{5}$$

where

$$E \equiv \left[I_1 \left(C_a^2, \frac{T_b}{T_{oa}}, \eta_R \right) - I_1 \left(C_a^2, \frac{T_b}{T_{oa}}, \eta_j \right) \right]$$
$$- \left[I_3 \left(C_a^2, \frac{T_b}{T_{oa}}, \eta_R \right) - I_3 \left(C_a^2, \frac{T_b}{T_{oa}}, \eta_j \right) \right] \equiv \left(1 - \frac{T_b}{T_{oa}} \right) I_2(\eta_j)$$

All the integrals and quantities mentioned above have been calculated on the Illiac* and have been tabulated and presented in graphical form (Ref. 7 and 9).

Local Characteristics within the Jet Mixing Region

In view of the fact that the treatment presented above was based on integral relations, lateral differentiations of the profiles to obtain

---

*Electronic digital computer, Engineering Research Laboratory, University of Illinois.

local properties are not recommended. The present analysis is again based on integral relations whenever possible.

Following a certain streamline at the ordinate y within such a jet mixing region, one would have from the continuity relationship that

$$\frac{d}{dx} \int_{y_j}^{y} \rho \; u dy = 0$$

which is equivalent to

$$\frac{d}{dx} \left(x \int_{\eta_j}^{\eta} \frac{\varphi}{\Lambda - C_a^2 \varphi^2} \; d\eta \right) = 0 \tag{6}$$

After the differentiation is carried out, the equation (6) goes into

$$I_1 (\eta) - I_1 (\eta_j) + \frac{d\eta}{dx} \left(\frac{x\varphi}{\Lambda - C_a^2 \varphi^2} \right) = 0$$

or

$$\frac{d\eta}{dx} = - \frac{[I_1(\eta) - I_1(\eta_j)] \; (\Lambda - C_a^2 \varphi^2)}{x\varphi} \tag{7}$$

which is a basic relation needed in this analysis. It describes the change of the dimensionless coordinate η pertaining to a certain stream filament as it proceeds downstream. It is obvious that the jet boundary streamline has the constant property values within the "fully developed mixing regions.

Selecting a control volume within such a jet mixing region such that the top control surface coincides with a streamline (see Fig. 1), the integral momentum relationship

$$\int_{-\infty}^{y} \rho u^2 \; dy - u_a \int_{y_j}^{y} \rho u \; dy = \int_{o}^{x} \tau_t \; dx$$

becomes after being differentiated with respect to x

$$\frac{d}{dx} \left[\int_{-\infty}^{y} \rho u^2 \; dy - u_a \int_{y_j}^{y} \rho u \; dy \right] = \tau_t$$

10

which is equivalent to

$$\tau_t = \frac{(1-C_a^2)\rho_a u_a^2}{\sigma} \frac{d}{dx}\left[x \int_{-\infty}^{\eta} \frac{\varphi^2}{\Lambda - C_a^2\varphi^2} d\eta - x \int_{\eta_j}^{\eta} \frac{\varphi}{\Lambda - C_a^2\varphi^2} d\eta \right] \quad (8)$$

Carrying out the differentiation, the equation (8) goes into

$$\frac{\tau_t \sigma}{\rho_a U_a^2} = (1 - C_a^2)\left[I_2(\eta) - (I_1(\eta) - I_1(\eta_j)) + \frac{(\varphi^2-\varphi) x}{\Lambda - C_a^2\varphi^2} \frac{d\eta}{dx} \right] \quad (9)$$

Defining the shear stress function τ by

$$\tau = \frac{\tau_t \sigma}{\rho_a u_a^2}$$

one obtains by substituting equation (7) into the equation (9):

$$\tau = (1 - C_a^2)\left[I_2(\eta) - \varphi (I_1(\eta) - I_1(\eta_j)) \right] \quad (10)$$

It is readily seen from the definition

$$\tau_t = \rho\, \epsilon\, \frac{\partial u}{\partial y} = \frac{\rho}{\rho_a}\, \epsilon\, \frac{\rho_a u_a \sigma}{x} \frac{d\varphi}{d\eta}$$

one can estimate the eddy diffusity ϵ with the help of equation (10) and obtain

$$\epsilon = \frac{\epsilon \sigma^2}{x u_a} = (\Lambda - C_a^2\varphi^2)\, e^{\eta^2} \sqrt{\pi}\, \left[I_2(\eta) - \varphi (I_1(\eta) - I_1(\eta_j)) \right] \quad (11)$$

which shows that at a location x, ϵ is certainly not constant along the y direction. Limited experimental results obtained for $C_a^2 = 0$ (Ref. 10) seem to support our analysis, see Figure 2a. While no experimental verification of the Mach Number influence or the temperature ratio effect is presently available, it is reasonable to assume that our analysis should again exhibit the correct trends.*

The derivative of the shear stress function is also given as

$$\frac{d\tau}{d\eta} = \frac{\partial \tau_t}{\partial y}\frac{x}{\rho_a u_a^2} = -(1-C_a^2)\left[I_1(\eta) - I_1(\eta_j) \right] \frac{d\varphi}{d\eta} \quad (12)$$

By use of the Reynold's Analogy for the case of unity turbulent Prandtl Number,

---

*It must be noted that our results are in strong disagreement with the speculations of Ting and Libby(Ref. 4).

$$\frac{\tau_t}{\rho_a u_a^2} = \frac{C_{f1}}{2} = St_\ell$$

and the identity

$$I_2(\eta) \equiv \frac{I_3(\eta) - \frac{T_b}{T_{oa}} I_1(\eta)}{1 - \frac{T_b}{T_{oa}}}$$

one may interpret equation (10) as

$$St_\ell \times \sigma = (1 - C_a^2) \left[\frac{I_3(\eta) - \frac{T_b}{T_{oa}} I_1(\eta)}{1 - \frac{T_b}{T_{oa}}} - \varphi \left\{ I_1(\eta) - I_1(\eta_j) \right\} \right]^* \quad (13)$$

A direct derivation of equation (13) by applying the energy balance is shown in the Appendix B.

The <u>local shear work</u> and <u>dissipation functions,</u> W_s, θ_D can be evaluated from the following expressions namely

$$W_s = \frac{\tau_t u\sigma}{\rho_a u_a^3} = (1 - C_a^2)\varphi \left[I_2(\eta) - \varphi \left\{ I_1(\eta) - I_1(\eta_j) \right\} \right] \quad (14)$$

and

$$\theta_D = \frac{\tau_t \frac{\partial u}{\partial y} x}{\rho_a u_a^3} = \frac{e^{-\eta^2}(1 - C_a^2)}{\sqrt{\pi}} \left[I_2(\eta) - \varphi \left\{ I_1(\eta) - I_1(\eta_j) \right\} \right] \quad (15)$$

---

*For $\eta = \eta_j$, $St \times \sigma \big|_{\eta_j} = (1 - C_a^2)\dfrac{I_3(\eta_j) - \frac{T_b}{T_{oa}} I_1(\eta_j)}{1 - \frac{T_b}{T_{oa}}}$

$$= (1 - C_a^2) \frac{E}{1 - \frac{T_b}{T_{oa}}} = (1 - C_a^2) I_2(\eta_j)$$

which represents the energy transfer across the streams and has been presented before (equation 2-3, in Ref. 1).

The integral $\int_{-\infty}^{y} \tau_t \frac{\partial u}{\partial y}\,dy$ represents the total rate of dissipation up to ordinate y in the mixing region and it is shown in the Appendix C that

$$\frac{\sigma \int_{-\infty}^{y} \tau_t \frac{\partial u}{\partial y}\,dy}{\rho_a u_a^3} = (1 - C_a^2)\,[\varphi\, I_2(\eta) - \frac{\varphi^2}{2}\left\{I_1(\eta) - I_1(\eta_j)\right\} - \frac{1}{2}\, I_4(\eta)] \qquad (16)$$

For y approaches infinity, one would obtain Φ, the total time <u>rate of dissipation</u> of mechanical energy per unit length along the mixing region (with unit thickness) which is given by

$$\Phi = \frac{\sigma \int_{-\infty}^{\infty} \tau_t \frac{\partial u}{\partial y}\,dy}{\rho_a u_a^3} = \frac{(1 - C_a^2)}{2}\,[I_2(\eta_R) - I_4(\eta_R)]* \qquad (17)$$

where the relationship

$$I_2(\eta_R) = I_1(\eta_R) - I_1(\eta_j)$$

has been introduced.

The <u>velocity component v</u> in the y direction can also be obtained for such a jet mixing region. In Appendix D, it is shown that the v component measured in the reference system of coordinates (X, Y) is given by

$$\sigma\, \varphi' = \varphi\,(\eta - \eta_m) - [I_1(\eta) - I_1(\eta_j)] \qquad (18)$$

where
$$\varphi' = \frac{v}{u_a}$$

---

*Note that this is essentially the integral mechanical energy relationship

$$\frac{\partial}{\partial x} \int_{y_j}^{\infty} \rho u\, \frac{u_a^2}{2}\,dy - \frac{\partial}{\partial x} \int_{-\infty}^{\infty} \frac{\rho u^3}{2}\,dy = \int_{-\infty}^{\infty} u\,\left(\frac{\partial u}{\partial y}\right)^2 dy$$

which can be derived by integrating along the y direction the equation of motion for such a constant pressure jet mixing region after being multiplied by the velocity.

Evaluations of all these functions and integrals introduced above have been carried out on the Illiac for five parametric values of $\frac{T_b}{T_{oa}}$, $(\frac{T_b}{T_{oa}} = 0.1, 0.5, 1, 2, 5)$ at five values of Crocco Number $(C_a^2 = 0, 0.2, 0.4, 0.6, 0.8)$.

The distribution of the shear stress function τ and the eddy diffusivity function ε are presented in Fig. 2 for three values of $\frac{T_b}{T_{oa}}$ at various Crocco Numbers. In Fig. 2a, experimental results of limited amount for isoenergetic $(\frac{T_b}{T_{oa}} = 1)$ incompressible flow $(C_a^2 = 0)$ obtained by hot wire measurements (ref. 6) are also shown. The agreement between the theoretical calculations and the experimental results are reasonably good.

The distribution of shear work and dissipations functions W_s θ_D are presented in Fig. 3. The total time rate of dissipation of mechanical energy in such jet mixing regions is presented in Fig. 4 while the distribution of vertical component of the velocity (v-component) within the jet mixing region is presented in Fig. 5.

Department of Mechanical and Industrial Engineering
Engineering Experiment Station
University of Illinois
Urbana, Illinois
July 1962

Appendix A

Discussion of the Similarity Parameter σ
in the Turbulent Jet Mixing Region

In a fully-developed jet mixing region with $Pr_t = 1$, the Similarity parameter σ can best be related to the change in slope of the inflection point tangent of the velocity profile. Selecting the established "erf-function" profile in such a mixing region, one can obtain by differentiation

$$\frac{d\varphi}{d\eta} = \frac{1}{\sqrt{\pi}} \, e^{-\eta^2}$$

so that for the inflection point of the velocity profile, $\eta = 0$, one would obtain

$$\left.\frac{d\varphi}{d\eta}\right)_{\eta=0} = \frac{1}{\sqrt{\pi}}$$

Within the x, y system of coordinates one may determine, for the stations, x_1 and x_2 the maximum slope of the velocity profile,

$$\left.\frac{\partial u}{\partial y}\right|_{max}^{(x)} \quad \text{and obtain}$$

$$\sigma = \frac{\sqrt{\pi}\,(x_2 - x_1)}{u_a \left[\dfrac{1}{\left.\dfrac{\partial u}{\partial y}\right|_2} - \dfrac{1}{\left.\dfrac{\partial u}{\partial y}\right|_1} \right]}$$

As $\dfrac{x_2}{x_1}$ becomes large, a stationary value is obtained for σ (fully developed profile)

$$\sigma \to \frac{\sqrt{\pi}}{u_a} \times \left.\frac{\partial u}{\partial y}\right|_x$$

The value of σ has been well established for the isoenergetic incompressible flow case to be $\sigma = 12$, and the relation of $\sigma = 12 + 2.758M$ has been also suggested by Korst and Tripp (ref. 11) to account for the effect of compressibility.

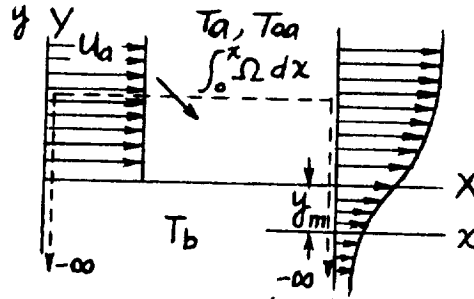## Energy Transport within the Turbulent Jet Mixing Region

Fig. (B-1)

Selecting a control volume as shown in the Fig. B-1 such that the top control surface coincides with a streamline considered, the integral energy relationship

$$\int_{-\infty}^{y} \rho u C_p T_o \, dy - C_p T_{oa} \int_{y_j}^{y} \rho u \, dy - C_p T_b \int_{-\infty}^{y_j} \rho u \, dy = \int_{o}^{x} \Omega \, dx$$

gives

$$\frac{d}{dx} \left[\int_{-\infty}^{y} \rho u C_p T_o \, dy - C_p T_{oa} \int_{y_j}^{y} \rho u \, dy - C_p T_b \int_{-\infty}^{y_j} \rho u \, dy \right] = \Omega \quad (B-1)$$

As

$$\int_{-\infty}^{y} \rho u C_p T_o \, dy = \frac{x \rho_a u_a C_p T_{oa} \, (1 - C_a^2)}{\sigma} \int_{-\infty}^{\eta} \frac{\Lambda \, \varphi}{\Lambda - C_a^2 \varphi^2} \, d\eta$$

$$C_p T_{oa} \int_{y_j}^{y} \rho u \, dy = \frac{x \rho_a u_a C_p T_{oa} \, (1 - C_a^2)}{\sigma} \int_{\eta_j}^{\eta} \frac{\varphi}{\Lambda - C_a^2 \varphi^2} \, d\eta$$

$$C_p T_b \int_{-\infty}^{y_j} \rho u \, dy = \frac{x \rho_a u_a C_p T_{oa} \, (1 - C_a^2)}{\sigma} \frac{T_b}{T_{oa}} \int_{-\infty}^{\eta_j} \frac{\varphi}{\Lambda - C_a^2 \varphi^2} \, d\eta$$

16

Equ. (B-1) becomes

$$\Omega = \frac{C_p T_{oa} \rho_a u_a (1 - C_a^2)}{\sigma} \left[I_3(\eta) - \left\{ I_1(\eta) - I_1(\eta_j) \right\} \right.$$

$$+ x \left(\frac{\Lambda \varphi}{\Lambda - C_a^2 \varphi^2} - \frac{\varphi}{\Lambda - C_a^2 \varphi^2} \right) \left(- \frac{I_1(\eta) - I_1(\eta_j) (\Lambda - C_a^2 \varphi^2)}{x \varphi} \right)$$

$$\left. - I_1(\eta_j) \frac{T_b}{T_{oa}} \right]$$

which can be reduced to

$$\frac{\Omega \sigma}{C_p T_{oa} \rho_a u_a} = (1 - C_a^2) [I_3(\eta) - \Lambda \left\{ I_1(\eta) - I_1(\eta_j) \right\} - \frac{T_b}{T_{oa}} I_1(\eta_j)] \quad \text{(B-2)}$$

With the definition for Stanton Number

$$St_\ell = \frac{\Omega}{C_p \rho_a u_a (T_{oa} - T_b)}$$

and the relation

$$\Lambda = \frac{T_b}{T_{oa}} + (1 - \frac{T_b}{T_{oa}}) \varphi$$

which holds for unity Prandtl Number, the equ. (B-2) will change into

$$St_\ell \sigma = (1 - C_a^2) \left[\frac{I_3(\eta) - \frac{T_b}{T_{oa}} I_1(\eta)}{1 - \frac{T_b}{T_{oa}}} - \varphi \left\{ I_1(\eta) - I_1(\eta_j) \right\} \right]$$

which is exactly the Equ. (13).

Appendix C

Derivation of Equation (16)

Starting from the Equ. (10)

$$\tau = \frac{\tau_t \, \sigma}{\rho_a u_a^2} = (1 - c_a^2)\,[I_2\,(\eta) - \varphi\left\{I_1\,(\eta) - I_1\,(\eta_j)\right\}]$$

one can see that

$$\int_{-\infty}^{y} \tau_t \frac{\partial u}{\partial y}\,dy = \frac{\rho_a u_a^3(1 - c_a^2)}{\sigma} \int_{\varphi=0}^{\varphi} \left[I_2(\eta) - \varphi\left\{I_1(\eta) - I_1(\eta_j)\right\}\right]\,d\varphi \quad (C-1)$$

This integral on the right hand side of the equ. (C-1) can be evaluated as follows:

$$\int_{\varphi=0}^{\varphi} [I_2\,(\eta) - \varphi\left\{I_1\,(\eta) - I_1\,(\eta_j)\right\}]\,d\varphi$$

$$= \left\{\varphi\left[\int_{-\infty}^{\eta} \frac{\varphi^2}{\Lambda - c_a^2 \varphi^2}\,d\eta - \varphi\int_{\eta_j}^{\eta} \frac{\varphi}{\Lambda - c_a^2 \varphi^2}\,d\eta\right]\right\}_{\varphi=0,\ \eta=-\infty}^{\varphi,\ \eta}$$

$$-\left\{\int_{-\infty}^{\eta} \frac{\varphi^3}{\Lambda - c_a^2 \varphi^2}\,d\eta - \int_{-\infty}^{\eta}[\varphi\int_{\eta_j}^{\eta}\frac{\varphi}{\Lambda - c_a^2\varphi^2}\,d\eta]\,d\varphi - \int_{-\infty}^{\eta}\frac{\varphi^3}{\Lambda - c_a^2\varphi^2}\,d\eta\right\}$$

$$= \varphi\, I_2\,(\eta) - \varphi^2\left\{I_1(\eta) - I_1(\eta_j)\right\} - \int_{-\infty}^{\eta}(\varphi\int_{\eta_j}^{\eta}\frac{\varphi}{\Lambda - c_a^2\varphi^2}\,d\eta)\,d\varphi$$

Also

$$\int_{-\infty}^{\eta} \left(\varphi \int_{\eta_j}^{\eta} \frac{\varphi}{\Lambda - C_a^2 \varphi^2} \, d\eta \right) d\varphi$$

$$= \left(\frac{\varphi^2}{2} \int_{\eta_j}^{\eta} \frac{\varphi}{\Lambda - C_a^2 \varphi^2} \, d\eta \right)_{\varphi = 0, \ \eta = -\infty}^{\varphi, \eta} - \int_{-\infty}^{\eta} \frac{\frac{\varphi^3}{2}}{\Lambda - C_a^2 \varphi^2} \, d\eta$$

$$= \frac{\varphi^2}{2} [I_1(\eta) - I_1(\eta_j)] - \frac{1}{2} I_4(\eta)$$

Equation (C-1) can be brought into the form

$$\frac{\sigma \int_{-\infty}^{y} \tau_t \frac{\partial u}{\partial y} \, dy}{\rho_a u_a^3} = (1 - C_a^2) \left[\varphi I_2(\eta) - \varphi^2 \left\{ I_1(\eta) - I_1(\eta_j) \right\} \right.$$

$$\left. + \frac{\varphi^2}{2} \left(I_1(\eta) - I_1(\eta_j) - \frac{1}{2} I_4(\eta) \right) \right]$$

$$= (1 - C_a^2) \left[\varphi I_2(\eta) - \frac{\varphi^2}{2} (I_1(\eta) - I_1(\eta_j)) - \frac{1}{2} I_4(\eta) \right]$$

which is equation (16).

Appendix D

The v-Component of the Velocity within the Jet Mixing Region

From the defining relationship of the intrinsic coordinate system, namely

$$X = x$$

$$Y = y - y_m$$

one obtains by following a certain fluid element in the reference system of coordinates

$$\frac{dY}{dX} = \frac{dY}{dx} = \frac{dy}{dx} - \frac{dy_m}{dx} \qquad (D-1)$$

As

$$\frac{dY}{dX} = \frac{v}{u} = \frac{\varphi'}{\varphi} \qquad (D-2)$$

Where $\varphi' = \dfrac{v}{u_a}$ with v the velocity component in the Y-direction measured in the reference system of coordinates

$$\frac{d\eta}{dx} = \frac{d\left(\sigma \frac{Y}{x}\right)}{dx} = \frac{\sigma}{x} \left[\frac{dy}{dx} - \frac{y}{x} \right] \qquad (D-3)$$

and

$$\frac{dy_m}{dx} = \frac{\eta_m}{\sigma} \qquad (D-4)$$

one combines the Equations (D-1) (D-2) (D-3) (D-4) with the additional relationship given by Equation (7) and obtains

$$\sigma \varphi' = \varphi (\eta - \eta_m) - [I_1 (\eta) - I_1 (\eta_j)] (\Lambda - C_a^2 \varphi^2)* \qquad (D-5)$$

The distributions of the v-component of the velocity are plotted in Figures 5a,b,c for various values of free stream Crocco Numbers and stagnation temperature ratios across the mixing region.

---

*   Note that the dimensionless velocity components for the x, y system and the X, Y system are related by

$$\varphi(X, Y) = \varphi(x,y)$$

$$\varphi'(X,Y) = \varphi'(x,y) - \varphi(x,y) \eta_m$$

REFERENCES

1. Korst, H. H., Chow, W. L., and Zumwalt, G. W., "Research On Transonic and Supersonic Flow of a Real Fluid at Abrupt Increases in Cross-Section, (With Special Consideration of Base Drag Problem)", University of Illinois, ME-TN-392-5, OSR-TR-60-74, Contract AF 18(600)-392, Dec., 1959.

2. Schlicting, H., "Boundary Layer Theory, "McGraw-Hill Book Co., New York, 1960.

3. Pai, S. I., "Fluid Dynamics of Jets", Van Nostrand Co., Inc., Princeton, N. J., 1954.

4. Ting, L., and Libby, P., "Remarks on the Eddy Viscosity in Compressible Mixing Flows", Journal of the Aero/Space Sciences, Vol. 27, No. 10, 1960.

5. Korst, H. H., Page, R. H., and Childs, M. E., "Compressible Two-Dimensional Jet-Mixing at Constant Pressure", University of Illinois, ME-TN-392-1, OSR-TN-54-82, Contract No. AF18 (600)-392, April, 1955.

6. Golik, R. J., "On Dissipative Mechanism Within Separated Flow Regions (with Special Consideration to Energy Transfer Across Turbulent, Compressible $Pr_t = 1$, Mixing Regions)", Ph.D. Thesis, University of Illinois, 1962.

7. Korst, H. H., Page, R. H., and Childs, M. E., "Compressible Two-Dimensional Jet Mixing at Constant Pressure-Tables of Auxiliary Functions for Fully Developed Mixing Profiles", University of Illinois, ME-TN-392-3, OSR-TN-55-99. Contract No. AF18(600)-392, April, 1955.

8. Page, R. H., and Korst, H. H., "Non-Isoenergetic Turbulent Compressible Jet Mixing With Consideration of its Influence on the Base Pressure Problem", Transactions of the Fourth Midwestern Conference on Fluid Mechanics, Purdue University, September, 1955.

9. Korst, H. H., and Chow, W. L., "Compressible Non-Isoenergetic Two-Dimensional Turbulent ($Pr_t = 1$) Jet Mixing at Constant Pressure-Auxiliary Integrals – Heat Transfer and Friction Coefficients for Fully Developed Mixing Profiles", University of Illinois, ME-TN-392-4, OSR-TN-59-380, Contract No. AF18(600)-392, January, 1959.

10. Mueller, T. J., "On Separation, Reattachment and Redevelopment of Turbulent Boundary Layers", Ph.D. thesis, University of Illinois, Department of Mechanical Engineering, 1961.

11. Korst, H. H., and Tripp, W., "The Pressure On a Blunt Trailing Edge Separating Two Supersonic Two-Dimensional Air Streams of Different Mach Number and Stagnation Pressure But Identical Stagnation Temperature", Proc. of the Fifth Midwestern Conference on Fluid Mechanics, 1957.
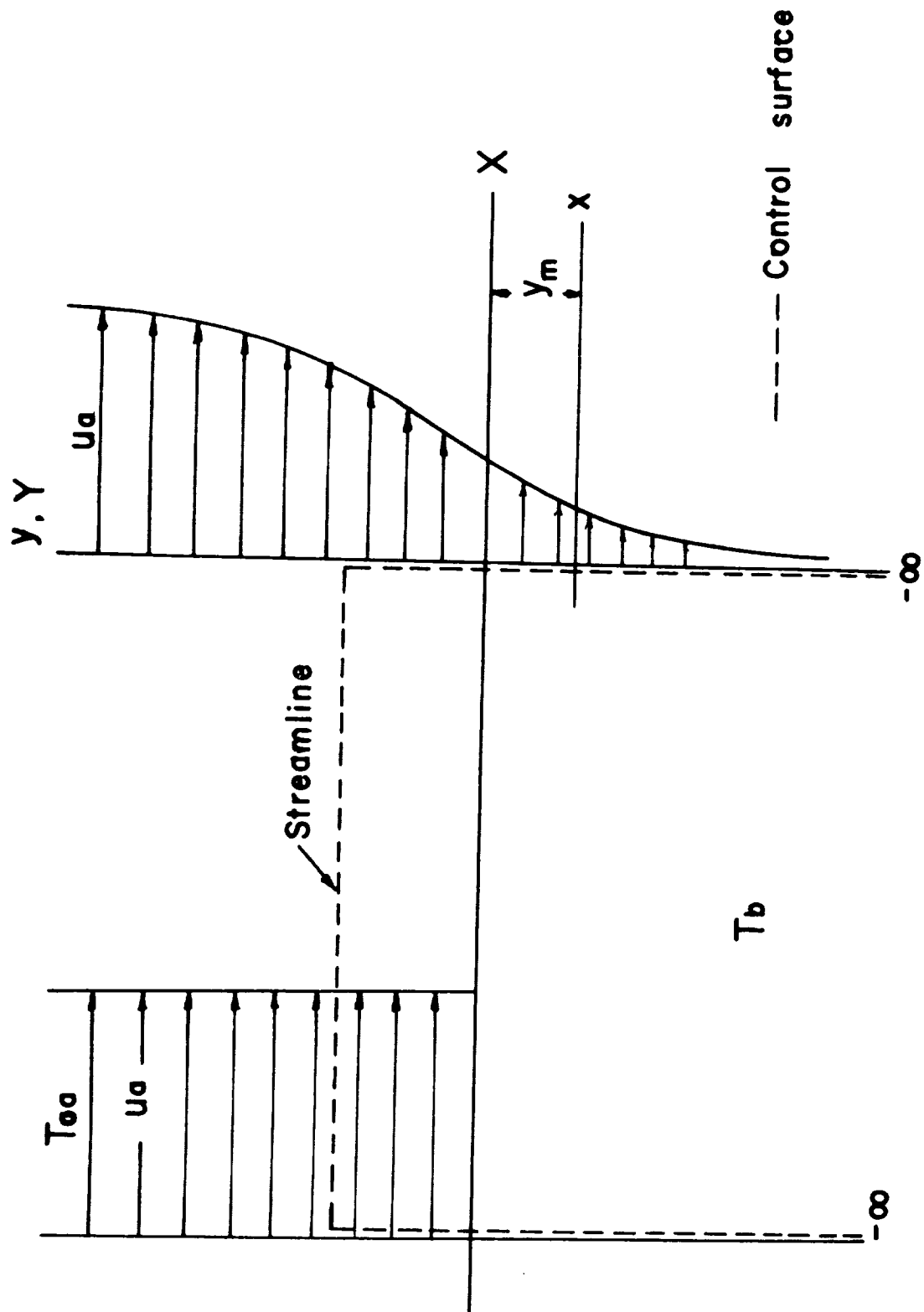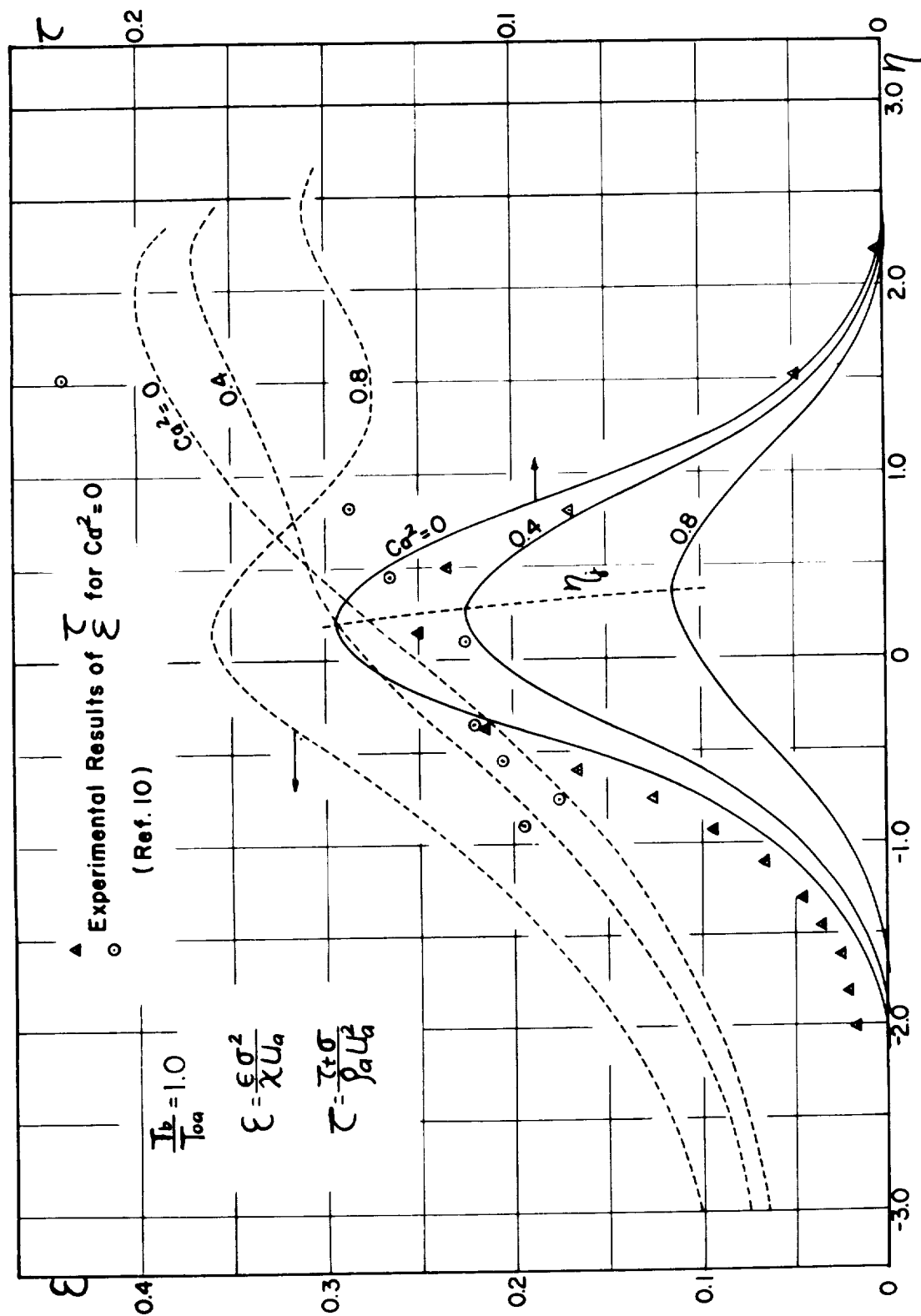
Fig. 1 The Jet Mixing Region

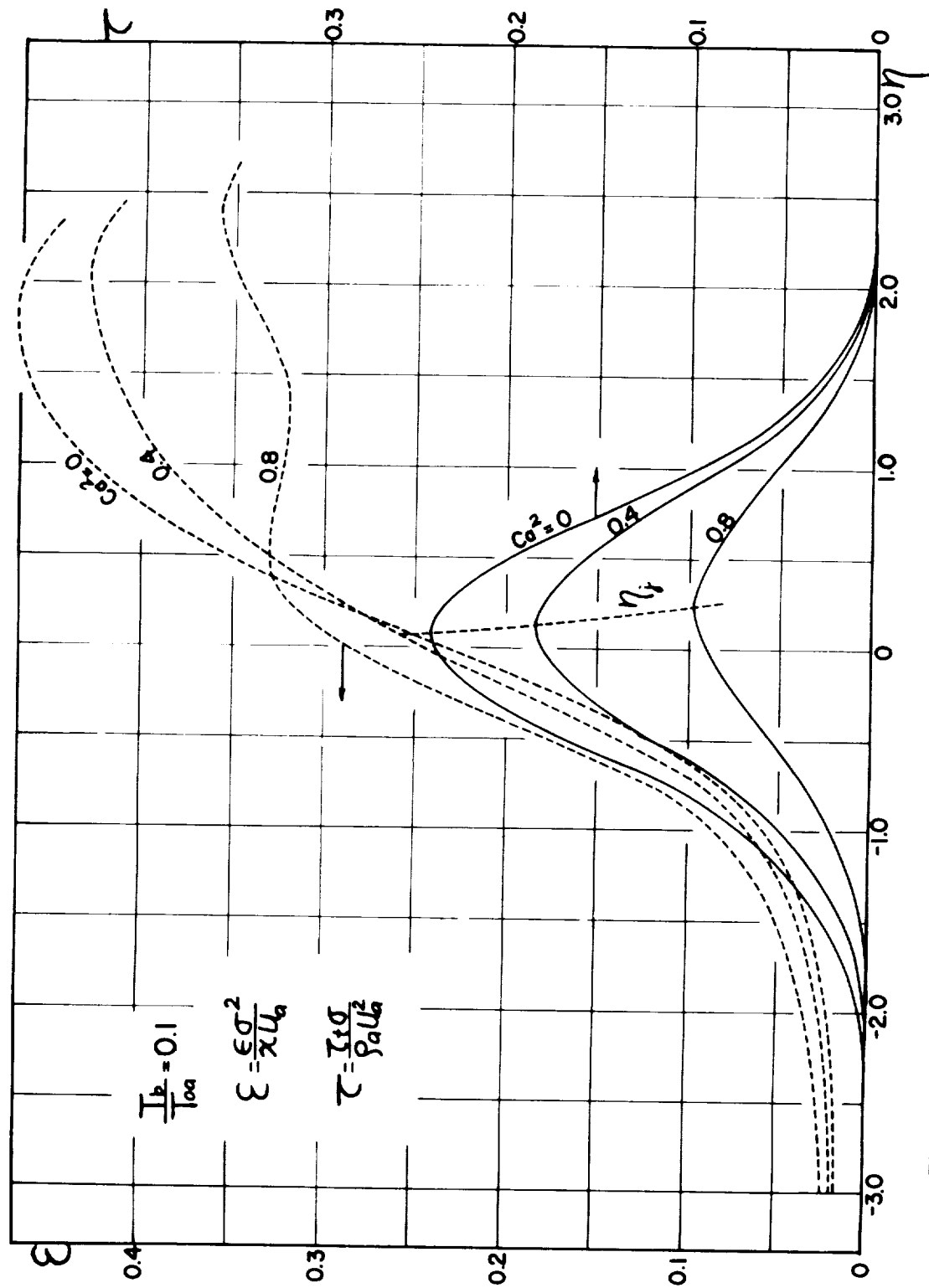Fig. 2a The Distribution of Shear Stress and Eddy Diffusivity Functions for $T_b/T_{oa} = 1.0$

Fig. 2b The Distribution of Shear Stress and Eddy Diffusivity Functions for $T_b/T_{oa} = 0.1$
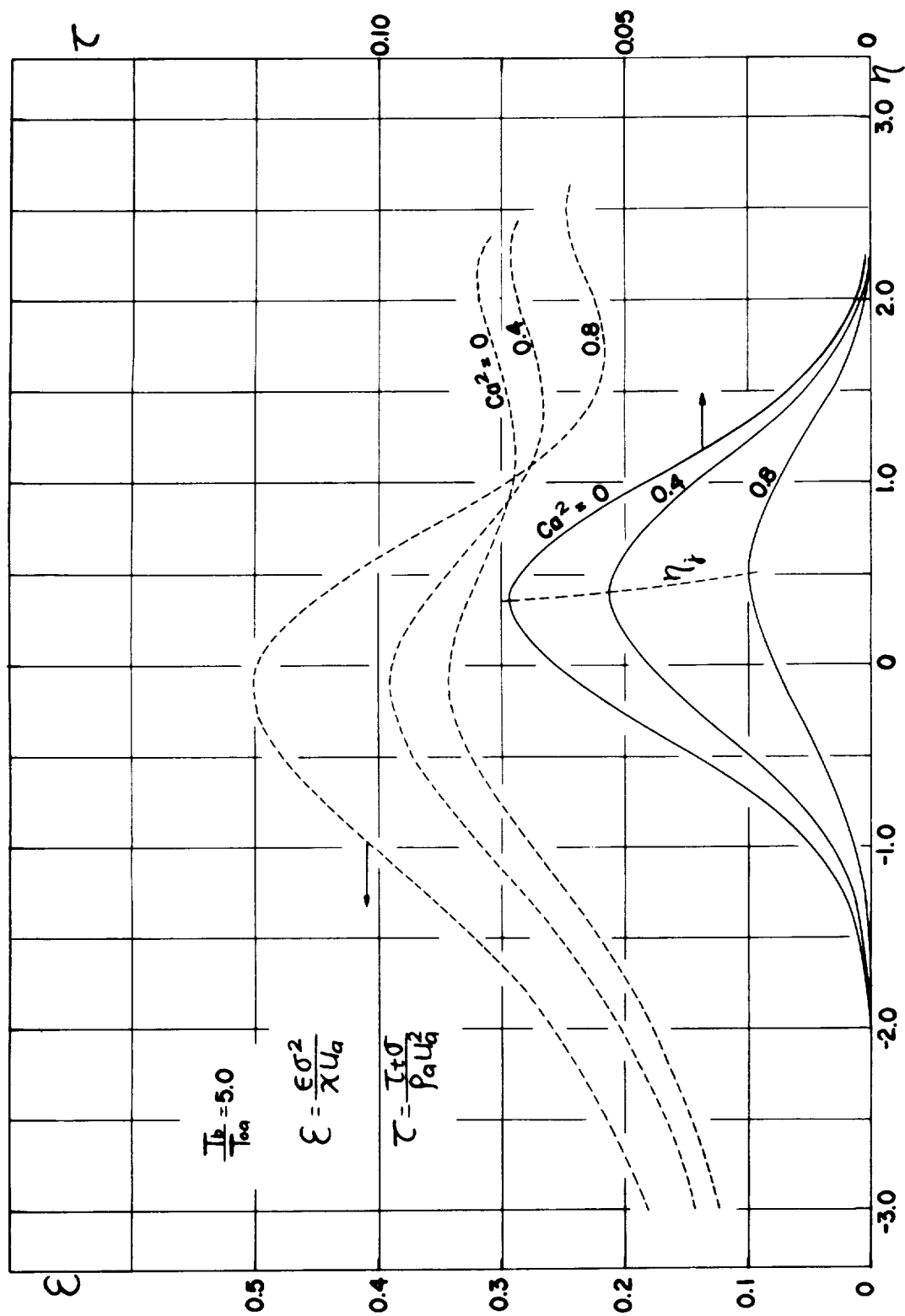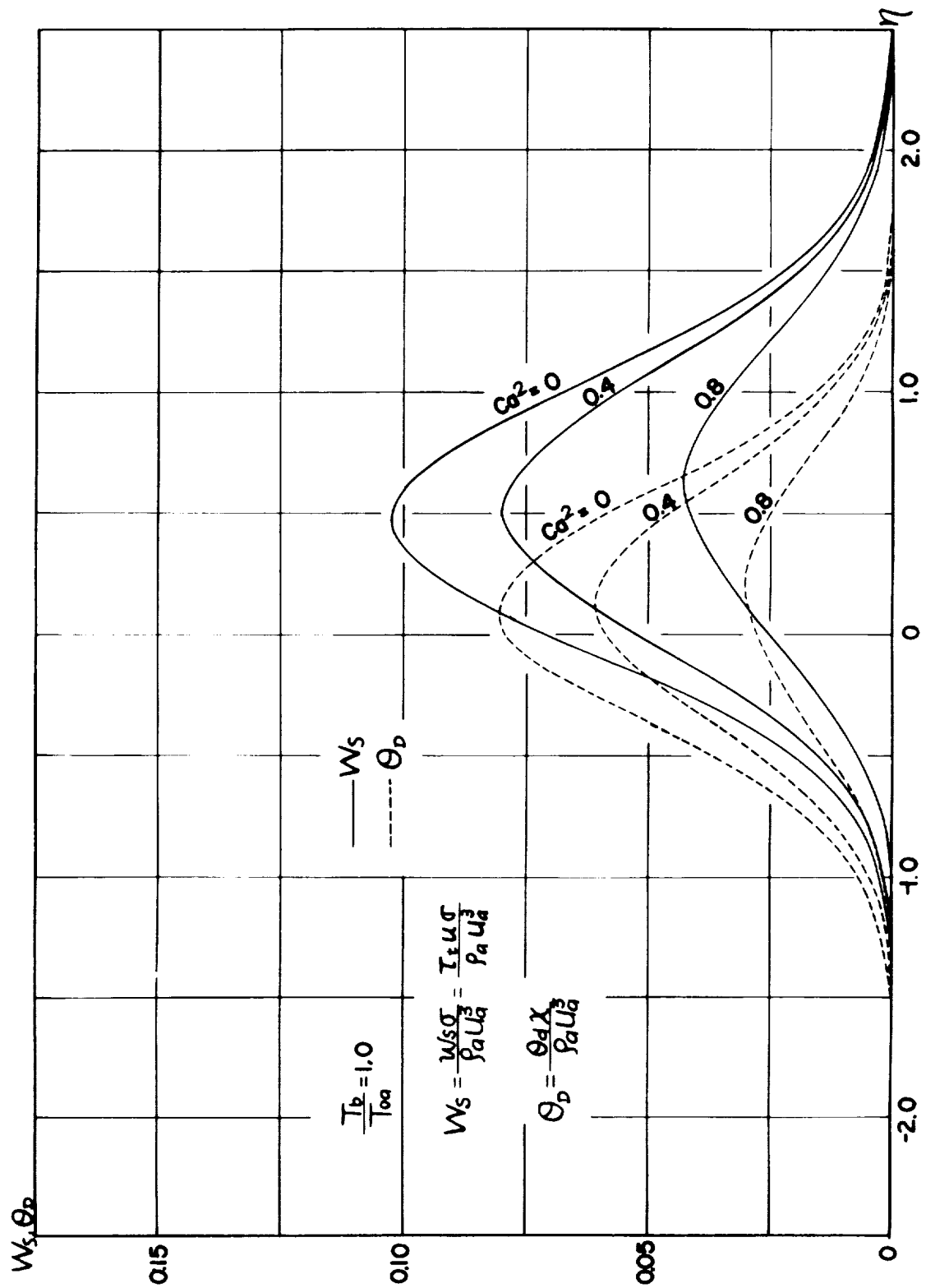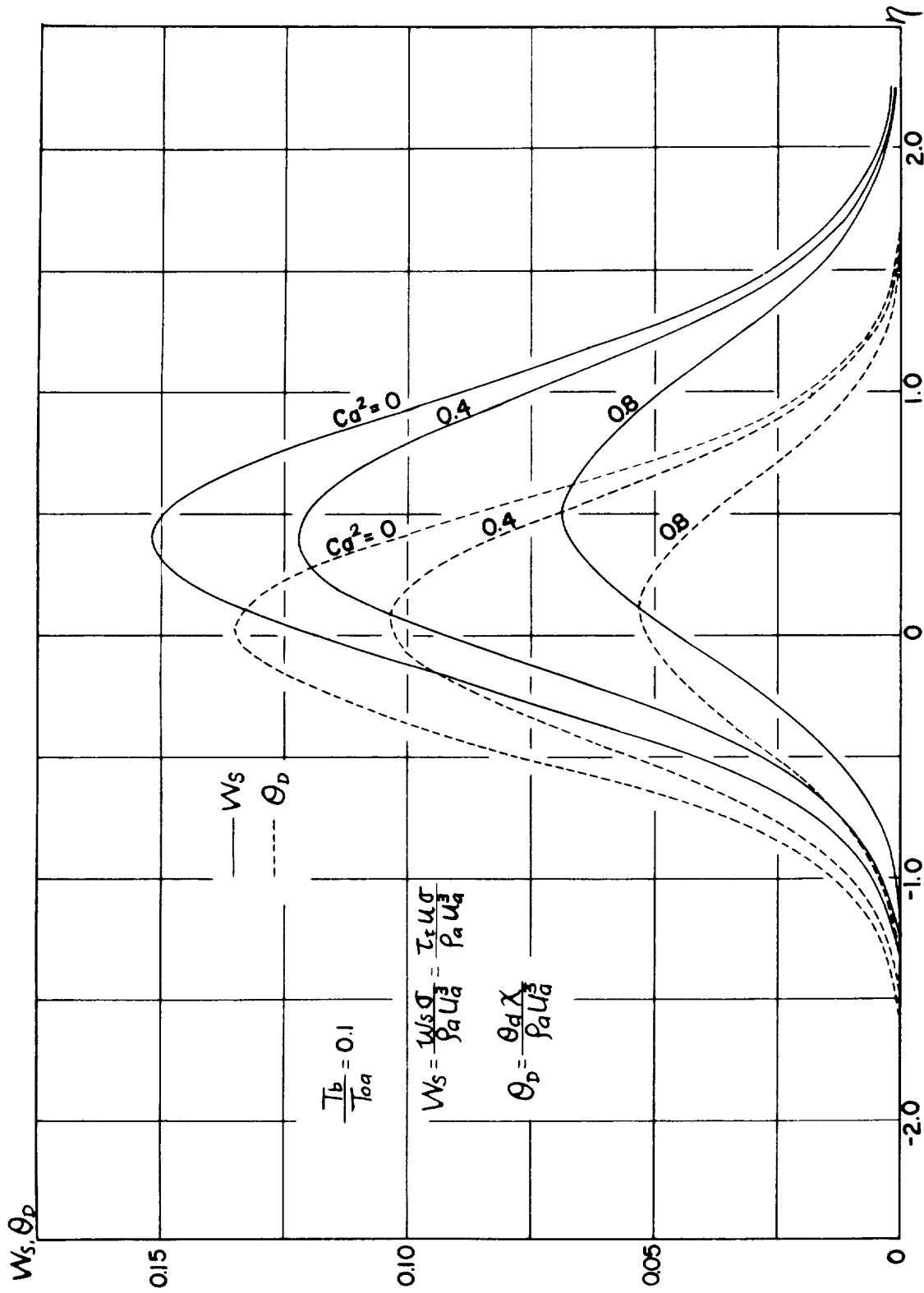
$\dfrac{T_b}{T_{oa}} = 0.1$

$\epsilon = \dfrac{\epsilon \sigma^2}{x u_a}$

$\tau = \dfrac{\tau_t \sigma}{\rho_a u_a^2}$

Fig. 2c The Distribution of Shear Stress and Eddy Diffusivity Functions for $T_b/T_{oa} = 5.0$

$$\frac{T_b}{T_{oa}} = 5.0$$

$$\epsilon = \frac{\epsilon \sigma^2}{\chi U_a}$$

$$\tau = \frac{\mathcal{T}_t \sigma}{\rho_a U_a^2}$$

25

$\dfrac{T_b}{T_{oa}} = 1.0$

$W_s = \dfrac{W_s \sigma}{\rho_a U_a^3} = \dfrac{\tau_t u \sigma}{\rho_a U_a^3}$

$\Theta_D = \dfrac{\Theta_d \chi}{\rho_a U_a^3}$

W_s ———

Θ_D - - - - -

$C\sigma^2 = 0$ 0.4 0.8

$C\sigma^2 = 0$ 0.4 0.8

Fig. 3a The Distribution of Shear Work and Dissipation Functions for $T_b/T_{oa} = 1.0$

26

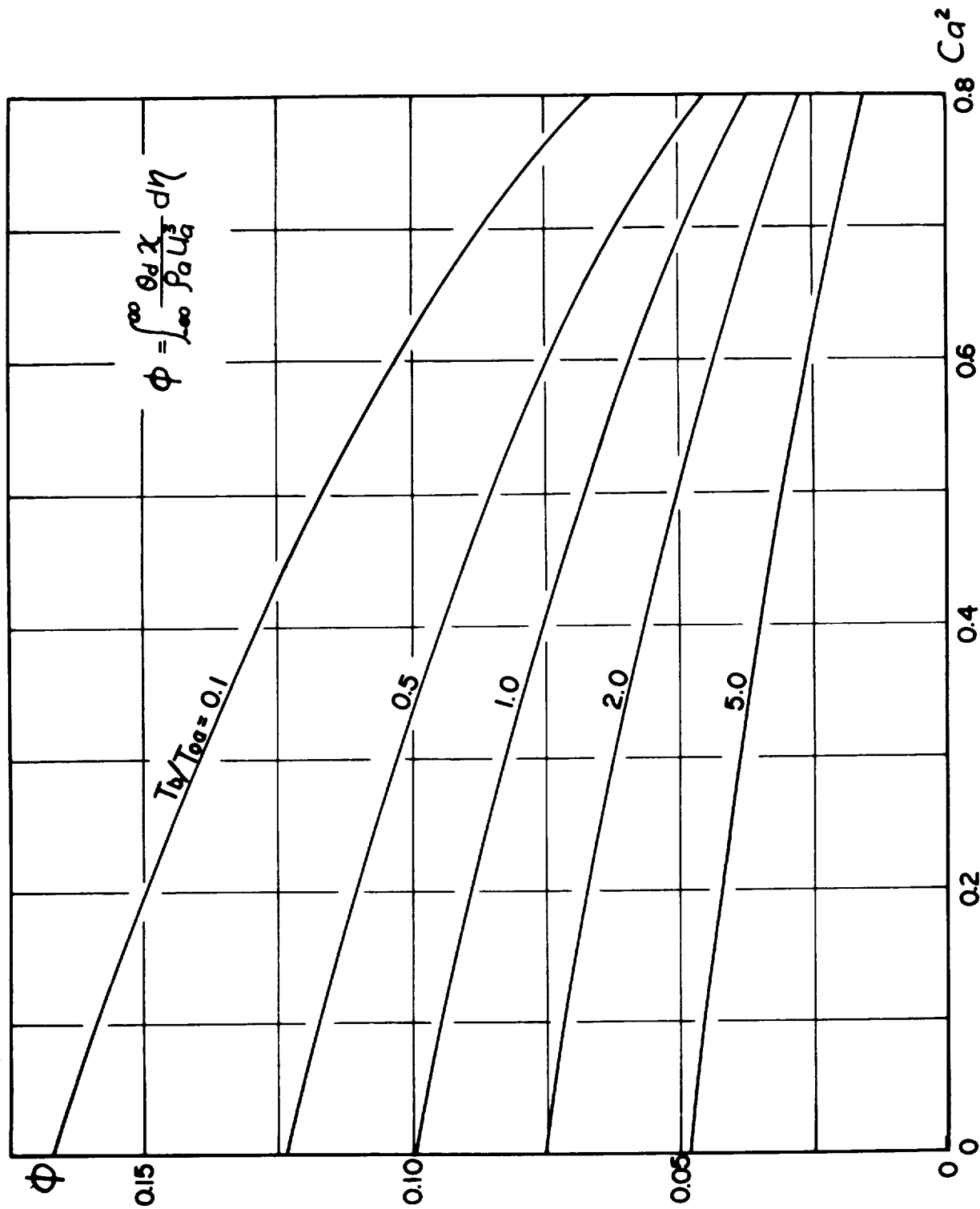Fig. 3b The Distribution of Shear Work and Dissipation Functions for $T_b/T_{oa} = 0.1$

27
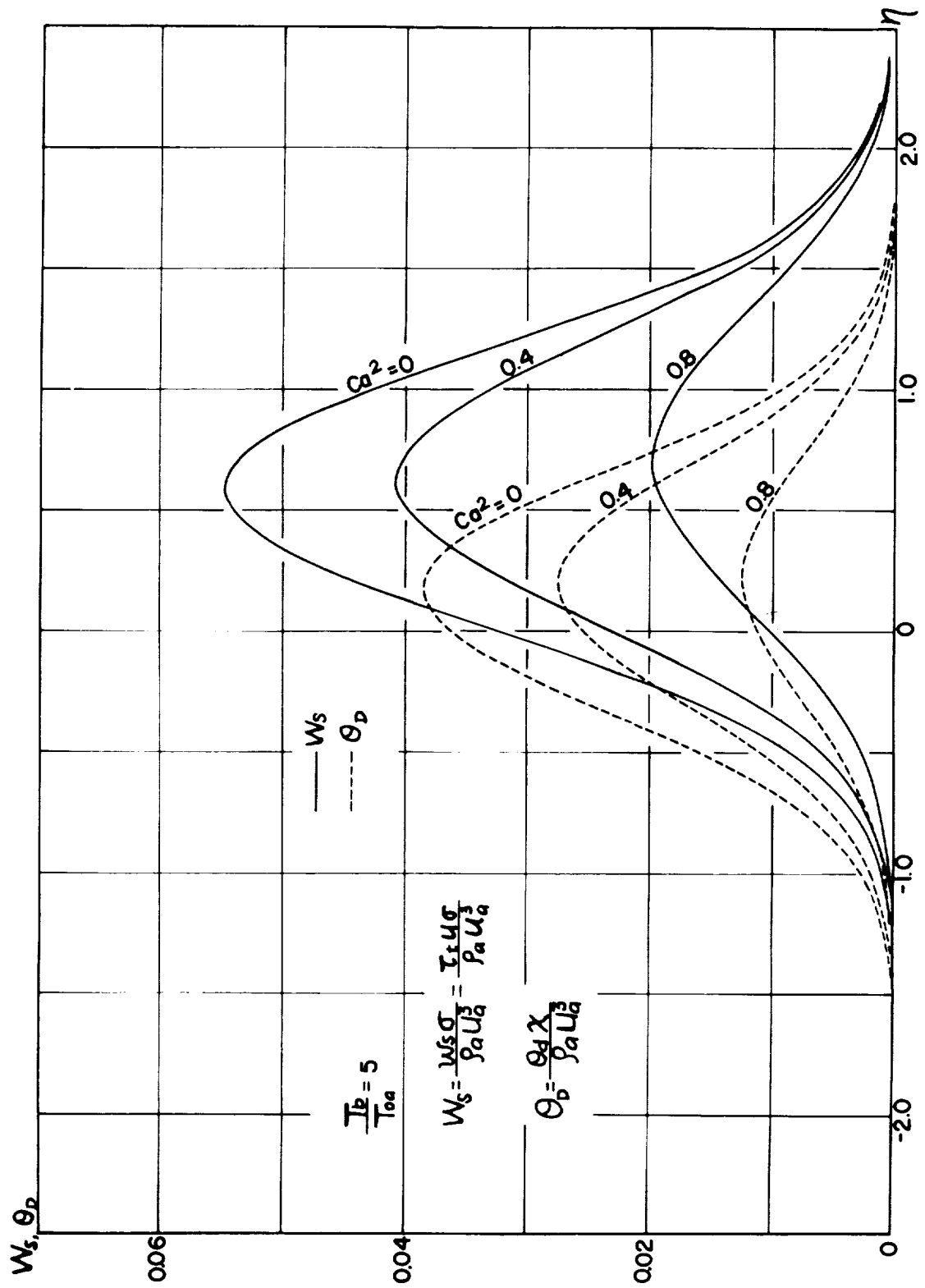
Fig. 3c   The Distribution of Shear Work and Dissipation Functions for T_b/T_{oa} = 5.0

28

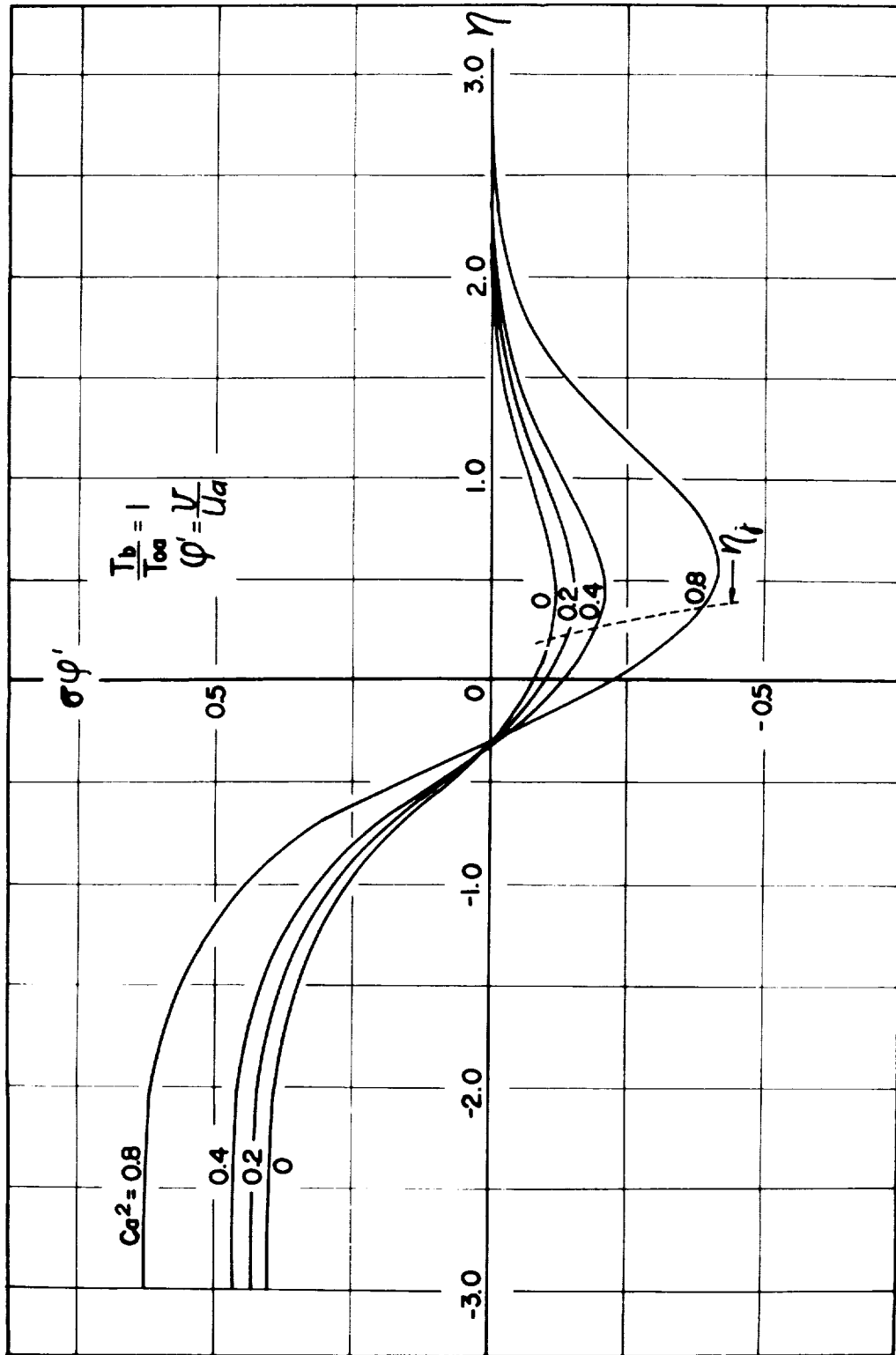Fig. 4   The Total Rate of Dissipation of Mechanical Energy in the Jet Mixing Region

Fig. 5a The Distribution of the v-Component of the Velocity for $T_b/T_{oa} = 1.0$
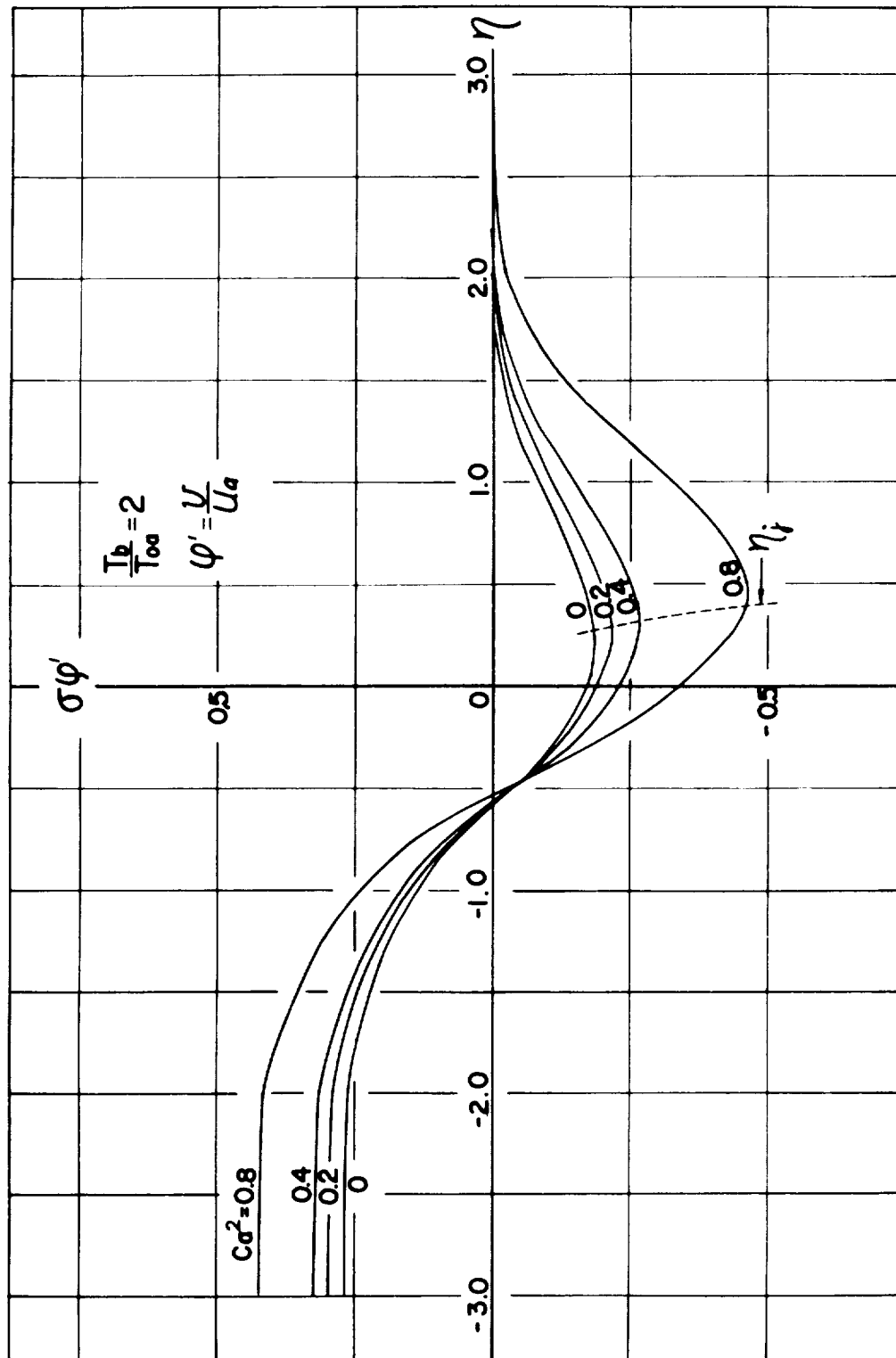
30

Fig. 5c   The Distribution of the v-Component of the Velocity for $T_b/T_{oa} = 2.0$
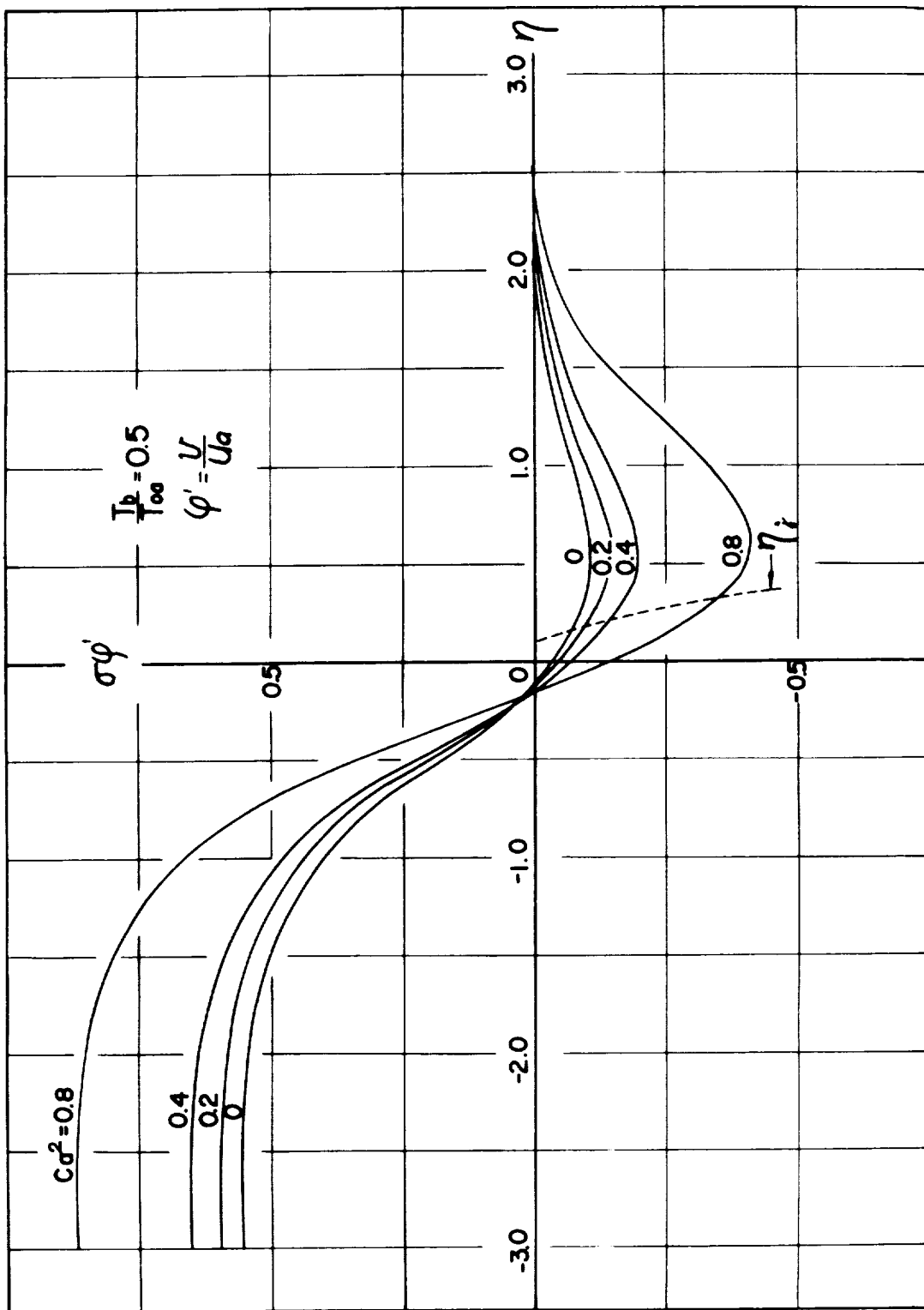
Fig. 5b The Distribution of the v-Component of the Velocity for $T_b/T_{oa} = 0.5$